Laser and Particle Beams (2017), *35*, 379–385.

doi:10.1017/S026303461700026X

Laser second-harmonic generation from an overdense plasma slab

M. KAUR,[1] P. C. AGARWAL,[2] AND S. KAUR[1]

[1]Department of Physics, Guru Nanak Dev University, Amritsar 143005, India
[2]Regional Institute of Education, Ajmer 305004, India

(RECEIVED 12 January 2017; ACCEPTED 4 April 2017)

Abstract

A s-polarized short-pulse laser impinged obliquely on an overdense plasma slab is shown to produce very significant second harmonic in the direction of specular reflection and transmission. The laser induces a non-linear current on electrons, which is curl free. However, with sharp plasma boundary, it gives rise to electromagnetic radiation at the second harmonic. Our formalism includes multiple reflections of the incident and second-harmonic waves from both the front and rear surfaces. The present work includes finiteness of the slab. The normalized second-harmonic amplitude acquires a sharp peak at some specific angle of incidence for a particular set of parameters dependent on thickness of the slab and plasma density.

Keywords: Laser–plasma interaction; Oblique incidence; Overdense plasma slab; Second-harmonic generation

1. INTRODUCTION

At high laser intensities the interaction between a laser beam and plasma, gives rise to a variety of non-linear effects (Marklund & Shukla, 2006; Ganeev *et al.*, 2012; Weber & Riconda, 2015; Zhang *et al.*, 2015). These include harmonic generation (HG) (Upadhyay & Tripathi, 2005), wakefield acceleration (Ibbotson *et al.*, 2010), THz (terahertz) radiation generation (Kumar *et al.*, 2011), and parametric instabilities (Klimo & Tikhonchuk, 2013). HG has its applications in the diagnostic of non-linear medium, coherent multiphoton spectroscopy, and other phenomena (Döbele *et al.*, 2000; Pirozhkov *et al.*, 2006; Li *et al.*, 2011; Liu *et al.*, 2011). Much of the work on HG in laser-produced plasma has been reported by thin foils (Teubner *et al.*, 2004), slab (Deb & Saha, 2015), gas jet (Banerjee *et al.*, 2003), and solid target (Dollar *et al.*, 2013). Some serious problems are encountered for HG from gaseous plasma, which encourages the researcher to use other targets. Increased value of laser intensity will increase harmonic intensity in gaseous plasma, cause rapid ionization of gaseous atoms, and decrease the harmonic emission. On the other hand, mismatch of the phase velocity of the laser beam and harmonic radiation affects the conversion efficiency. In a thin foil, harmonics have been mainly observed in reflection from the front side of massive solid targets. Efficiency of the yield can be increased by phase matching. It turns the process into a resonant one. Kaur and Sharma (2008) studied third HG in a laser-produced thin foil plasma with conversion efficiency obtained as 0.01%.

Currently, there is strong interest in intense short pulse laser interaction in plasma with ultrathin foils. One of the primary objectives is to achieve proton acceleration via TNSA (target normal sheath acceleration) or RPA (radiation pressure acceleration) mechanisms. In these studies, overdense plasma foils of thickness comparable with laser wavelength or much shorter wavelengths are employed (Tripathi *et al.*, 2009). Adusumilli *et al.* (2011) have argued that when a laser beam of finite spot size (e.g., a Gaussian beam) impinges on an ultrathin foil, the radiation pressure it exerts on the foil is more on the axis and decreases with distance r. As a result, the foil acquires a curvature. The laser falling on the curved boundary is no longer normal to the boundary. Optical ray makes an angle to the surface normal. Under such a situation transmission coefficients for the s and p polarizations are different and transmitted wave does not maintain its circular polarization. They showed that s-polarized laser obliquely impinged on a foil can give rise to second-harmonic generation (SHG) in the direction of specular reflection. Their treatment is limited to semi-infinite plasma. SHG of a right circularly polarized Gaussian electromagnetic beam in an unbounded magnetized plasma has been investigated by

Address correspondence and reprint requests to: S. Kaur, Department of Physics, Guru Nanak Dev University, Amritsar-143005, India. E-mail: sukhdeep.iitd@gmail.com

Kaur *et al.* (2009). Self-focusing of the laser beam increases the yield of HG. For normalized amplitude of the short pulse $eA_1/m\omega c = 0.3$, HG efficiency exceeding 1%. Kaur *et al.* (2010) have studied effect of self-focusing on resonant third HG for a Gaussian laser beam.

Singh and Gupta (2015) investigated the effect of self-focusing of a q-Gaussian laser beam on SHG in a preformed parabolic plasma channel by using moment theory approach. Harmonics yield increases with the increase in intensity of laser beam, plasma density, and channel depth. Purohit *et al.* (2013) have recently proposed SHG from a metallic thin film deposited over a glass half space. The laser is impinging obliquely on the film. The thin film has sufficiently high free carrier density, such that the harmonic is evanescent inside the film. They analyse the second harmonic in the reflected component and power conversion efficiency up to 10^{-5} has been obtained.

To overcome these limitations, overdense plasma came into play to generate higher order harmonics, which are free from phase-matching condition, results in higher harmonic order and intensity. Theoretical and experimentally studies have elucidated the two distinct processes, which are responsible for the HG from overdense plasma: coherent wakefield emission (CWE) and relativistic oscillating mirror (ROM) model. These both processes are very different although having a common origin, the Brunel process in which surface electrons, that is, Brunel electrons (Brunel, 1987) are first accelerated by laser field and then pushed back toward the plasma. In relativistic region, the ROM process dominates in which electrons are drawn out from the plasma surface. The critical surface from where the laser pulse reflects and oscillates with the velocity of light. During the period of laser-driving pulse, the phase of the reflected radiation redistributes due to the motion of the reflection point. This surface travels toward the laser due to which the pulse compresses causing the phase change leads to generation of high harmonics. A very fascinating experiment was performed by Streeter *et al.* (2011) with 50 fs laser pulse of intensity between 10^{17} and 10^{21} W/cm^2 incidents obliquely with p-polarization on aluminium target. They observed that for higher intensity $>10^{20}$ W/cm^2, the conversion efficiency of SHG was measured 22 ($\pm$8%). They compared the experimental results with ROM model and found that SHG efficiency depends on the intensity of the laser beam. Recently, Chen and Pukhov (2016) numerically simulated a scheme described by ROM model to produce bright high-order harmonics by controlling polarization.

In the sub-relativistic region, the CWE process dominates in which Brunel electrons come back to the plasma, some of them are temporally bunched and propagate across the density gradient of the plasma. As a consequence, the density gradient of the plasma accelerates and leads to generate electron plasma oscillations in their wake. These electrons are bunched temporally at the intervals of laser time period that excites the plasma frequencies resonantly which are multiples of the laser frequency. Consequently, harmonics are generated up to the plasma frequency related to maximum density of the target. Theoretical and experimental demonstration on high HG from overdense plasma with laser of moderate intensity is due to the CWE process given by Quere *et al.* (2006).

Teubner *et al.* (2004) have experimentally demonstrated the generation of harmonics in laser-produced plasma from rear and front side of the thin overdense foil. They used foil made up of carbon and aluminium, thickness ranging from 50 to 460 nm. As p-polarized laser obliquely incident on thin foil at incidence angle of 45°, harmonics are generated. They observed that fundamental harmonic as well as harmonics up to 10th order are transmitted from the rear side besides those from the front side. By increasing foil thickness, harmonic emission efficiency of the reflected harmonics increases as compared with the transmitted harmonics. They also found that as the polarization of incident laser beam changes from p to s with normal incidence, no harmonics are generated. The experimental observations are reproduced by particle-in-cell (PIC) simulations using one-dimensional LPIC code. An experimental study of fundamental and second harmonics from the rear side of thin overdense foil from ultrashort laser pulse is demonstrated by Eidmann *et al.* (2005). They examined the polarization properties, emission efficiencies and spectral shapes of the rear side harmonics. They found that p-polarized laser can generate significant rear side harmonics due to resonance absorption. The conversion efficiency enhances by increasing the laser intensity and reduces as the electron density increased in the foil. In these experiments, Brunel mechanism is responsible for the generation of harmonics from thin overdense foil. The rear side harmonic spectrum is broader than the incident laser light spectrum. The broadness of spectra increases with decreasing intensity and increasing foil thickness. This shows that duration of transmitted pulse is shorter than incident pulse. PIC simulation also supports the result.

In this paper, we study the generation of second harmonic of s-polarized laser from an overdense plasma slab, including multiple reflections of the incident as well as harmonic waves from both the front and rear surfaces. The second-harmonic ponderomotive force gives rise to electron oscillations at 2ω frequency, generating a second-harmonic current density. This current density is curl free in an uniform plasma and could produce only longitudinal field $\vec{E}_{2\omega}$. However, in the case of a bounded slab, it gives rise to appearance of space charges at the boundaries that lead to second-harmonic radiation on the reflection as well as transmission sides of the slab. Thus, sharp boundaries where electron density has large density gradient or a plasma with volume non-uniformity is essential for generating the harmonic.

In Section 2, we deduce an expression for non-linear current density due to s-polarized laser obliquely incident at an angle θ_i on an overdense plasma slab. Second-harmonic field is deduced in Section 3 followed by results and discussion in Section 4.

https://doi.org/10.1017/S026303461700026X Published online by Cambridge University Press

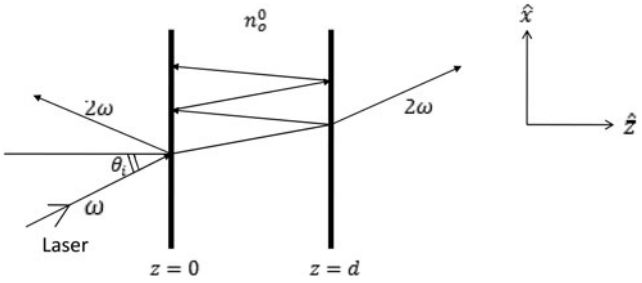

Fig. 1. Schematic presentation of SHG from a plasma slab.

2. NON-LINEAR CURRENT DENSITY

Consider a thin slab of overdense plasma of equilibrium electron density n_0^0 contained between $z = 0$ and $z = d$. A laser is obliquely incident from $z < 0$ side at angle of incidence θ_i (cf. Fig. 1) with electric and magnetic fields as,

$$\vec{E}_i = \hat{y}A_0 e^{-i(\omega t-(\omega/c)\cos\theta_i z-(\omega/c)\sin\theta_i x)}, \tag{1}$$

$$\vec{B}_i = \frac{A_0}{c}(-\cos\theta_i\hat{x} + \sin\theta_i\hat{z})e^{-i(\omega t-(\omega/c)\cos\theta_i z-(\omega/c)\sin\theta_i x)}, \tag{2}$$

where $\vec{k} = (\omega/c)\sin\theta_i\hat{x} + (\omega/c)\cos\theta_i\hat{z}$, c is the speed of light in vacuum.

Inside the plasma, the fields of the laser are,

$$\vec{E}_{II} = \hat{y}A_0\left[T_1 e^{ik_z z} + T_2 e^{-ik_z z}\right]e^{-i(\omega t-(\omega/c)\sin\theta_i x)}, \tag{3}$$

$$\vec{B}_{II} = \frac{A_0}{c}\left[(T_2 e^{-ik_z z} - T_1 e^{ik_z z})\frac{k_z c}{\omega}\hat{x} + (T_2 e^{-ik_z z} + T_1 e^{ik_z z})\sin\theta_i\hat{z}\right] \times e^{-i(\omega t-(\omega/c)\sin\theta_i x)}. \tag{4}$$

Following the conventional theory of linear reflection and transmission, we obtain

$$T_1 = \frac{2}{D_1}\left(1 + \frac{ck_z}{\omega\cos\theta_i}\right), \tag{5}$$

$$T_2 = -\frac{2}{D_1}\left(1 - \frac{ck_z}{\omega\cos\theta_i}\right)e^{2ik_z d}, \tag{6}$$

where

$$D_1 = \left[\left(1 + \frac{ck_z}{\omega\cos\theta_i}\right)^2 - \left(1 - \frac{ck_z}{\omega\cos\theta_i}\right)^2 e^{2ik_z d}\right].$$

The laser imparts oscillatory velocity to electrons, $\vec{v}_\omega = (e\vec{E}_{II}/mi\omega)$ and exerts second-harmonic ponderomotive force on them,

$$\vec{F}_{p2\omega} = -\frac{m}{2}\nabla(\vec{v}_\omega.\vec{v}_\omega).$$

$$\vec{F}_{p2\omega} = \frac{e^2A_0^2}{2m\omega^2}\left[\left(2i\frac{\omega}{c}\sin\theta_i\right)(T_1^2e^{2ik_z z} + T_2^2e^{-2ik_z z} + 2T_1T_2)\hat{x} + 2ik_z(T_1^2e^{2ik_z z} - T_2^2e^{-2ik_z z})\hat{z}\right]e^{-2i(\omega t-(\omega/c)\sin\theta_i x)}. \tag{7}$$

Using this in the equation of motion, we obtain the non-linear electron drift velocity at 2ω,

$$\vec{v}_{2\omega}^{NL} = -\frac{e^2A_0^2}{2m^2\omega^3}\left[\frac{\omega}{c}\sin\theta_i(T_1^2e^{2ik_z z} + T_2^2e^{-2ik_z z} + 2T_1T_2)\hat{x}. + k_z(T_1^2e^{2ik_z z} - T_2^2e^{-2ik_z z})\hat{z}\right]e^{-2i(\omega t-(\omega/c)\sin\theta_i x)}. \tag{8}$$

The equation of continuity yields the second-harmonic non-linear density perturbation,

$$n_{2\omega}^{NL} = -\frac{n_0^0e^2A_0^2}{2m^2\omega^4}\frac{\omega^2}{c^2}\left[\epsilon(T_1^2e^{2ik_z z} + T_2^2e^{-2ik_z z}). + 2T_1T_2\sin^2\theta_i\right]e^{-2i(\omega t-(\omega/c)\sin\theta_i x)}, \tag{9}$$

where $\epsilon = 1 - \omega_p^2/\omega^2$.

From the Poisson's equation, one obtains the second-harmonic field E_2, $\nabla\cdot\vec{E}_2 = -((e/\epsilon_0\epsilon_2)n_{2\omega}^{NL})$, where $\epsilon_2 = 1 - (\omega_p^2/4\omega^2)$, ϵ_0 is the free space permittivity.

The non-linear current density at second harmonic is given by,

$$\vec{J}_{2\omega}^{NL} = -n_0^0e\vec{v}_{2\omega}^{NL},$$

$$\vec{J}_{2\omega}^{NL} = \frac{n_0^0e^3A_0^2}{2m^2\omega^3} \times\left[\frac{\omega}{c}\sin\theta_i(T_1^2e^{2ik_z z} + T_2^2e^{-2ik_z z} + 2T_1T_2)\hat{x} + k_z(T_1^2e^{2ik_z z} - T_2^2e^{-2ik_z z})\hat{z}\right]e^{-2i(\omega t-(\omega/c)\sin\theta_i x)}. \tag{10}$$

3. SECOND-HARMONIC FIELD

The wave equation governing the second-harmonic field inside the plasma is,

$$\nabla^2\vec{E}_2 + \frac{4\omega^2 - \omega_p^2}{c^2}\vec{E}_2 = -i\frac{2\omega}{c^2\epsilon_0}\vec{J}_{2\omega}^{NL} + \nabla\left(-\frac{e}{\epsilon_0\epsilon_2}n_{2\omega}^{NL}\right). \tag{11}$$

The second harmonic propagates in the x–z plane with t, x dependence as,

$$\vec{E}_2 = \vec{F}_2(z)e^{-2i(\omega t-(\omega/c)\sin\theta_i x)}.$$

https://doi.org/10.1017/S026303461700026X Published online by Cambridge University Press

Equation (11) in component for simplifies to

$$\frac{\partial^2 F_2}{\partial z^2} + K_{2z}^2 F_2 = i\frac{\omega_p^2}{c^2} a_0 A_0 \sin\theta_i \times \left[(T_1^2 e^{2ik_z z} + T_2^2 e^{-2ik_z z})\left(\frac{\in}{\in_2} - 1\right) + 2T_1 T_2 \left(\frac{\sin\theta_i^2}{\in_2} - 1\right)\right]\hat{x} + i\frac{\omega_p^2}{c^2} a_0 A_0 \left(\frac{k_z c}{\omega}\right)[T_1^2 e^{2ik_z z} - T_2^2 e^{-2ik_z z}]\left(\frac{\in}{\in_2} - 1\right)\hat{z}.$$

The solution of x-component of wave equation is given by

$$F_{2X} = A_2^{\mathrm{I}}(T_1^2 e^{2ik_z z} + T_2^2 e^{-2ik_z z}) + A_2^{\mathrm{II}}(2T_1 T_2) + A_2^{\mathrm{III}} e^{ik_{2z} z} + A_2^{\mathrm{IV}} e^{-ik_{2z} z}. \quad (12)$$

The solution of the z-component of wave equation is

$$F_{2Z} = B_2^{\mathrm{I}}\left(T_1^2 e^{2ik_z z} - T_2^2 e^{-2ik_z z}\right) + B_2^{\mathrm{III}} e^{ik_{2z} z} + B_2^{\mathrm{IV}} e^{-ik_{2z} z}. \quad (13)$$

The constants are obtained as

$$A_2^{\mathrm{I}} = \frac{i}{3} a_0 A_0 \sin\theta_i \left(\frac{\epsilon}{\epsilon_2} - 1\right),$$

$$A_2^{\mathrm{II}} = i\frac{\omega_p^2}{c^2}\frac{a_0 A_0 \sin\theta_i}{k_{2z}^2}\left(\frac{\sin^2\theta_i}{\epsilon_2} - 1\right),$$

$$B_2^{\mathrm{I}} = i a_0 A_0 \left(\frac{k_z c}{\omega}\right)\left(\frac{\epsilon}{\epsilon_2} - 1\right). \quad (14)$$

The solution of the wave equation on reflection side of the slab ($z < 0$) can be written as,

$$F_{2X} = A_2 e^{-2i(\omega/c)\cos\theta_i z},$$

$$F_{2Z} = \frac{\sin\theta_i}{\cos\theta_i} A_2 e^{-2i(\omega/c)\cos\theta_i z}. \quad (15)$$

While on the transmission side $z > d$,

$$F_{2X} = B_2 e^{2i(\omega/c)\cos\theta_i z},$$

$$F_{2Z} = -\frac{\sin\theta_i}{\cos\theta_i} B_2 e^{2i(\omega/c)\cos\theta_i z}. \quad (16)$$

For complimentary system $\nabla \cdot E_2 = 0$, we get

$$B_2^{\mathrm{III}} = -\frac{2\omega}{c}\frac{\sin\theta_i}{k_{2z}} A_2^{\mathrm{III}},$$

$$B_2^{\mathrm{IV}} = \frac{2\omega}{c}\frac{\sin\theta_i}{k_{2z}} A_2^{\mathrm{IV}}. \quad (17)$$

Applying boundary conditions on tangential and axial component of electric field at interface $z = 0$ and $z = d$, we get,

$$A_2 = A_2^{\mathrm{I}}(T_1^2 + T_2^2) + A_2^{\mathrm{II}}(2T_1 T_2) + A_2^{\mathrm{III}} + A_2^{\mathrm{IV}},$$
$$\tan\theta_i A_2 = \epsilon_2 B_2^{\mathrm{I}}(T_1^2 - T_2^2) + \epsilon_2 B_2^{\mathrm{III}} + \epsilon_2 B_2^{\mathrm{IV}},$$
$$A_2^{\mathrm{I}}(T_1^2 e^{2ik_z d} + T_2^2 e^{-2ik_z d}) + A_2^{\mathrm{II}}(2T_1 T_2) + A_2^{\mathrm{III}} e^{ik_{2z} d} + A_2^{\mathrm{IV}} e^{-ik_{2z} d} = B_2 e^{2i(\omega/c)\cos\theta_i d},$$
$$\epsilon_2 B_2^{\mathrm{I}}(T_1^2 e^{2ik_z d} - T_2^2 e^{-2ik_z d}) + \epsilon_2 B_2^{\mathrm{III}} e^{ik_{2z} d} + \epsilon_2 B_2^{\mathrm{IV}} e^{-ik_{2z} d} = -\tan\theta_i B_2 e^{2i(\omega/c)\cos\theta_i d}.$$

Solving these equations, we obtain the second-harmonic amplitude in reflected and transmitted sides of the plasma slab,

$$A_2 = A_2^{\mathrm{I}}(T_1^2 + T_2^2) + A_2^{\mathrm{II}}(2T_1 T_2) - \frac{\alpha}{\beta} + \lambda\left[-4\frac{\epsilon_2}{\beta}\frac{\omega}{c}\frac{\sin\theta_i}{k_{2z}}\alpha\beta' e^{ik_{2z} d} + 4\epsilon_2\frac{\omega}{c}\frac{\sin\theta_i}{k_{2z}}\delta\right],$$

$$B_2 = [A_2^{\mathrm{I}}(T_1^2 e^{2ik_z d} + T_2^2 e^{-2ik_z d}) + A_2^{\mathrm{II}}(2T_1 T_2)]e^{-2i(\omega/c/)cos\theta_i d} + \left[\frac{\alpha\beta'\lambda}{\beta}\left\{tan\theta_i(e^{2ik_{2z} d} - 1) - \epsilon_2\frac{2\omega}{c}\frac{\sin\theta_i}{k_{2z}}(e^{2ik_{2z} d} + 1)\right\}\right] - \lambda\delta\left\{tan\theta_i(e^{ik_{2z} d} - e^{-ik_{2z} d}) - \left(\epsilon_2\frac{2\omega}{c}\frac{\sin\theta_i(e^{ik_{2z} d} + e^{-ik_{2z} d})}{k_{2z}}\right)\right\}e^{-2i(\omega/c)\cos\theta_i d} - \frac{\alpha}{\beta}e^{ik_{2z} d - i(2\omega/c)\cos\theta_i d},$$

where $\alpha = \tan\theta_i(A_2^{\mathrm{I}}(T_1^2 + T_2^2) + A_2^{\mathrm{II}}(2T_1 T_2)) - \epsilon_2 B_2^{\mathrm{I}}(T_1^2 - T_2^2)$, $\beta = \tan\theta_i + \epsilon_2 2\omega/c\,\sin\theta_i/k_{2z}$, $\beta' = \tan\theta_i - \epsilon_2\,2\omega/c\sin\theta_i/k_{2z}$, $\delta = \tan\theta_i\left[A_2^{\mathrm{I}}(T_1^2 e^{2ik_z d} + T_2^2 e^{-2ik_z d}) + A_2^{\mathrm{II}}(2T_1 T_2)\right] + \epsilon_2 B_2^{\mathrm{I}}(T_1^2 e^{2ik_z d} - T_2^2 e^{-2ik_z d})$, $\lambda = \dfrac{1}{\beta'^2 e^{ik_{2z} d} - \beta^2 e^{-ik_{2z} d}}$.

We have plotted normalized second-harmonic amplitude A_2/A_0 and B_2/B_0 with respect to angle of incidence θ_i, slab thickness, and plasma density. Figure 2 represents variation of normalized second-harmonic amplitude with angle of incidence in overdense plasma. The other parameters are: $a_0 = 0.3$, $\omega d/c = 5$, $\omega_p/\omega = 3$. At $\theta_i = 0$, the second harmonic is zero because current is normal to the plasma boundary and give rise to only space charge oscillations. At $\theta_i = \pi/2$, the laser penetration is too little inside the plasma, hence the HG vanishes. The yield of HG increases with the angle of incidence. It reaches maximum at $\theta_i \approx 50°$ and then decreases. The reflected amplitude peak is six times more than the transmitted amplitude peak. Figure 3

https://doi.org/10.1017/S026303461700026X Published online by Cambridge University Press

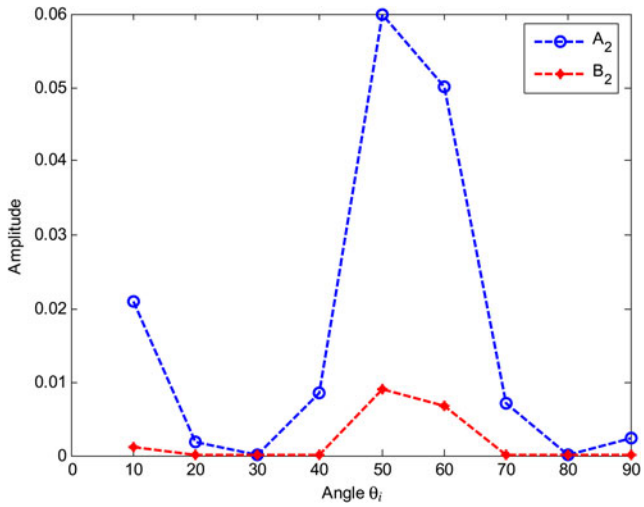

Fig. 2. Normalized second-harmonic amplitude versus angle of incident in overdense plasma. The parameters are $a_0 = 0.3$, $\omega d/c = 5$, $\omega_p/\omega = 3$.

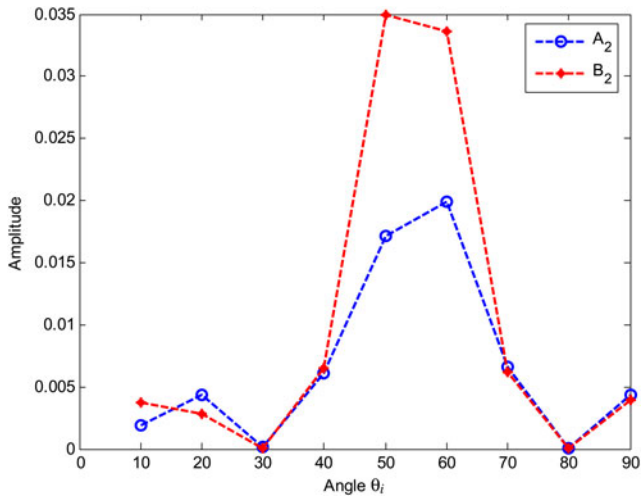

Fig. 3. Normalized second-harmonic amplitude versus angle of incident in underdense plasma. The parameters are $a_0 = 0.3$, $\omega d/c = 5$, $\omega_p/\omega = 0.7$.

represents the variation of second-harmonic amplitude from an underdense plasma slab for $\omega_p/\omega = 0.7$ and other parameters are same as Figure 2. Reflection side overdense plasma gives stronger SHG. However, for the transmission side underdense plasma is strong. This is because the plasma is transparent for the wave propagation, although the second-harmonic amplitude at transmission side is observed more than twice of an order of magnitude. The main motivation is indeed overdense plasma, although underdense plasma is studied for the sake of comparison and completeness.

Figure 4 represents the variation of second-harmonic amplitude with the thickness of the slab for the overdense plasma. The other parameters are $\omega_p/\omega = 3$, $\theta_i = 50°$, and $a_0 = 0.3$. As we increases the thickness of the slab, the second harmonic on the reflection side initially increases and then saturates, where as in the transmission side, it

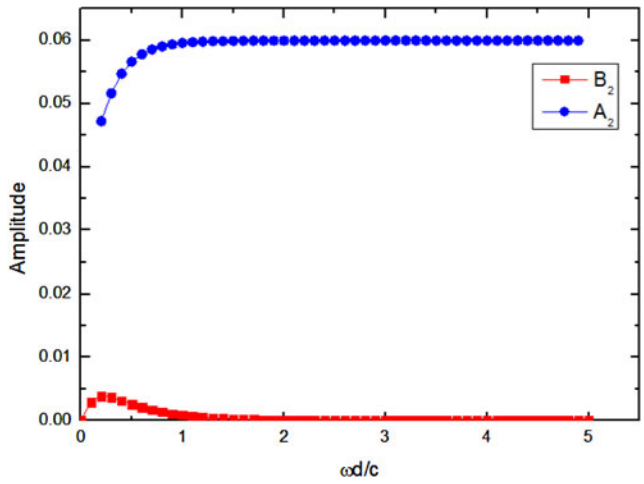

Fig. 4. Normalized second-harmonic amplitude versus thickness of plasma slab for overdense plasma. The parameters are $a_0 = 0.3$, $\omega_p/\omega = 3$, $\theta_i = 50°$.

initially increases then decreases and as the thickness of the slab increases, it tends to zero. Figure 5 represents the variation of second-harmonic amplitude versus thickness of the plasma slab in underdense plasma. The other parameters are $\omega_p/\omega = 0.7$, $\theta_i = 50°$, and $a_0 = 0.3$. Oscillating behavior is observed for SHG on the reflected side. This is primarily due to the superposition of forward and backward propagating fundamental (ω frequency) waves inside the slab. However, in transmission side the yield of SHG increases and tends to saturates, when we increase the thickness of the slab, this is because due to continuous wave propagation.

Figure 6 represents the variation of normalized second harmonics with normalized plasma density. The other parameters are $\omega d/c = 5$, $\theta_i = 50°$, and $a_0 = 0.3$. As the plasma density increases, the yield of second harmonic increases in both the reflected and the transmission sides. At $\omega_p/\omega = 2$,

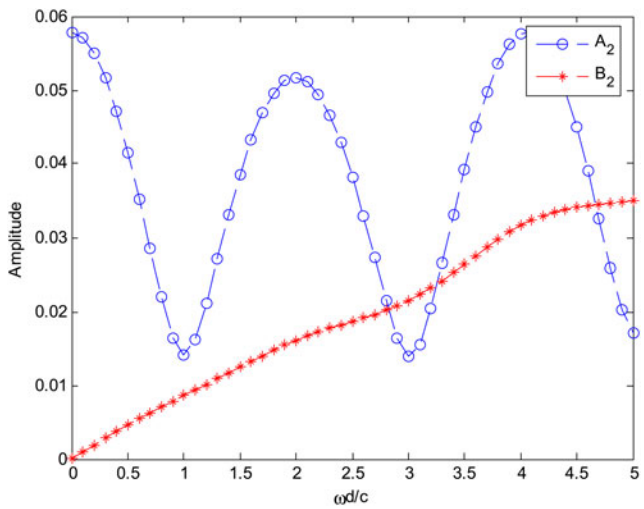

Fig. 5. Normalized second-harmonic amplitude versus thickness of plasma slab for underdense plasma. The parameters are $a_0 = 0.3$, $\omega_p/\omega = 0.7$, $\theta_i = 50°$.

https://doi.org/10.1017/S026303461700026X Published online by Cambridge University Press

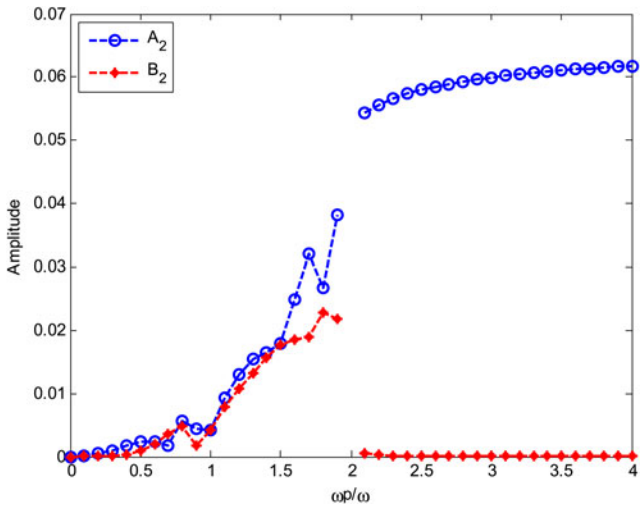

Fig. 6. Normalized second-harmonic amplitude versus plasma density. The parameters are $a_0 = 0.3$, $\omega d/c = 5$ and $\theta_i = 50°$.

there is resonant enhancement in the yield as the space charge oscillations induced by the ponderomotive force are resonantly enhanced. The singularity is masked by collisions. Beyond the singularity, the second-harmonic yield increases on the reflected side. However, due to higher plasma density, the wave does propagate in the transmission side, hence the yield is smaller.

4. DISCUSSION

An intense laser obliquely incident on an overdense thin slab plasma produces very significant second harmonic on the reflection as well as transmission sides. The yield of HG increases with the angle of incidence. For the parameters $a_0 = 0.3$, $\omega d/c = 5$, $\omega_p/\omega = 3$, and at incident angle $\theta_i = 0$, the second harmonic is zero because it gives rise to only space charge oscillations. It reaches maximum at $\theta_i \approx 50°$ and then decreases, both in the reflection and transmission sides of the slab. The intensity of transmitted second harmonic is smaller than that of the reflected harmonic. Thickness of the slab also affects the yield of HG. In the overdense case, reflection amplitude saturates for higher thickness, whereas transmission amplitude vanishes for $\omega_p/\omega = 2$, as the second-harmonic wave becomes evanescent and very little second harmonic reaches the rear side. Oscillating behavior is observed for underdense plasma slab. However, in transmission side the yield of SHG tends to saturates, because the wave can continue to propagate. The main motivation is indeed overdense plasma, although underdense plasma is studied for the sake of comparison and completeness. Plasma density with optimum angle of incidence also affects the yield of SHG. At $\omega_p/\omega = 2$, there is resonant enhancement in the yield as the space charge oscillation induced by the ponderomotive force are resonantly enhanced.

ACKNOWLEDGMENTS

The author is grateful to UGC-sanctioned UGC-BSR Research Start-Up-Grant No. F. 20-23(12)/2012(BSR) for supporting financially for the numerical computations. They are grateful to Professor V. K. Tripathi for simulating and useful discussion.

REFERENCES

Adusumilli, K., Goyal, D. & Tripathi, V. K. (2011). Relativistic second harmonic generation from an *S*-polarized laser in overdense plasma. *Phys. Plasmas* **18**, 083105.

Banerjee, S., Valenzuela, A. R., Shah, R. C., Maksimchuk, A. & Umstadter, D. (2003). High-harmonic generation in plasmas from relativistic laser-electron scattering. *J. Opt. Soc. Am. B* **20**, 182–190.

Brunel, F. (1987). Not-so-resonant, resonant absorption. *Phys. Rev. Lett.* **59**, 52–55.

Chen, Z. Y. & Pukhov, A. (2016). Bright high-order harmonic generation with controllable polarization from a relativistic plasma mirror. *Nat. Commun.* **7**, 12515.

Deb, S. & Saha, A. (2015). Fractional quasi phase matched broadband second harmonic generation in a tapered zinc telluride slab using total internal reflection considering the effect of nonlinear law of reflection. *Optik* **126**, 3371–3375.

Döbele, H. F., Czarnetzki, U. & Goehlich, A. (2000). Diagnostics of atoms by laser spectroscopic methods in plasmas and plasma-wall interaction studies (vacuum ultraviolet and two-photon techniques). *Plasma Sources Sci. Technol.* **9**, 477–491.

Dollar, F., Cummings, P., Chvykov, V., Willingale, L., Vargas, M., Yanovsky, V., Zulick, C., Maksimchuk, A., Thomas, A. G. R. & Krushelnick, K. (2013). Scaling high-order harmonic generation from laser-solid interactions to ultrahigh intensity. *Phys. Rev. Lett.* **110**, 175002.

Eidmann, K., Kawachi, T., Marcinkevičius, A., Bartlome, R., Tsakiris, G. D., Witte, K. & Teubner, U. (2005). Fundamental and harmonic emission from the rear side of a thin overdense foil irradiated by an intense ultrashort laser pulse. *Phys. Rev. E* **72**, 036413.

Ganeev, R. A., Hutchison, C., Witting, T., Frank, F., Okell, W. A., Zaïr, A., Weber, S., Redkin, P. V., Lei, D. Y., Roschuk, T., Maier, S. A., L'opez-Quintás, I., Martín, M., Castillejo, M., Tisch, J. W. G. & Marangos, J. P. (2012). High-order harmonic generation in graphite plasma plumes using ultrashort laser pulses: A systematic analysis of harmonic radiation and plasma conditions. *J. Phy. B: At. Mol. Opt. Phys.* **45**, 165402.

Ibbotson, T. P. A., Bourgeois, N., Rowlands-Rees, T. P., Caballero, L. S., Bajlekov, S. I., Walker, P. A., Kneip, S., Mangles, S. P. D., Nagel, S. R., Palmer, C. A. J., Delerue, N., Doucas, G., Urner, D., Chekhlov, O., Clarke, R. J., Divall, E., Ertel, K., Foster, P. S., Hawkes, S. J., Hooker, C. J., Parry, B., Rajeev, P. P., Streeter, M. J. V. & Hooker, S. M. (2010). Laser-wakefield acceleration of electron beams in a low density channel. *Phys. Rev. Spec. Top. Accel. Beams* **13**, 031301.

Kaur, S. & Sharma, A. K. (2008). Resonant third harmonic generation in a laser produced thin foil plasma. *Phys. Plasmas* **15**, 102705.

Kaur, S., Sharma, A. K. & Salih, H. A. (2009). Resonant second harmonic generation of a Gaussian electromagnetic beam in a collisional magnetoplasma. *Phys. Plasmas* **16**, 042509.

https://doi.org/10.1017/S026303461700026X Published online by Cambridge University Press

Kaur, S., Yadav, S. & Sharma, A. K. (2010). Effect of self-focusing on resonant third harmonic generation of laser in a rippled density plasma. *Phys. Plasmas* **17**, 053101.

Klimo, O. & Tikhonchuk, V. T. (2013). Laser-plasma interaction studies in the context of shock ignition: The regime dominated by parametric instabilities. *Plasma Phys. Control. Fusion* **55**, 095002.

Kumar, G., Pandey, S., Cui, A. & Nahata, A. (2011). Planar plasmonic terahertz waveguides based on periodically corrugated metal films. *N. J. Phys*. **13**, 033024.

Li, C., Zhou, M. L., Ding, W. J., Du, F., Liu, F., Li, Y. T., Wang, W. M., Sheng, Z. M., Ma, J. L., Chen, L. M., Lu, X., Dong, Q. L., Wang, Z. H., Lou, Z., Shi, S. C., Wei, Z. Y. & Zhang, J. (2011). Effects of laser-plasma interactions on terahertz radiation from solid targets irradiated by ultrashort intense laser pulses. *Phys. Rev. E* **84**, 036405.

Liu, Y., Durand, M., Houard, A., Forestier, B., Couairon, A. & Mysyrowicz, A. (2011). Efficient generation of third harmonic radiation in air filaments: A revisit. *Opt. Commun*. **284**, 4706–4713.

Marklund, M. & Shukla, P. K. (2006). Nonlinear collective effects in photon-photon and photon-plasma interactions. *Rev. Mod. Phys*. **78**, 1–47.

Pirozhkov, A. S., Bulanov, S. V., Esirkepov, T. Z., Mori, M., Sagisaka, A. & Daido, H. (2006). Attosecond pulse generation in the relativistic regime of the laser-foil interaction: The sliding mirror model. *Phys. Plasmas* **13**, 013107.

Purohit, P. K., Agrawal, V. K., Sharma, H. & Parashar, J. (2013). Second harmonic generation from a metallic thin film by an obliquely incident laser. *Phys. Scr*. **87**, 045403.

Quere, F., Thaury, C., Monot, P., Dobosz, S. & Martin, Ph. (2006). Coherent wake emission of high-order harmonics from overdense plasma. *Phy. Rev. Lett*. **96**, 125004.

Singh, A. & Gupta, N. (2015). Second harmonic generation by relativistic self-focusing of q-Gaussian laser beam in performed parabolic plasma channel. *Phys. Plasmas* **22**, 013102.

Streeter, M. J. V., Foster, P. S., Cameron, F. H., Borghesi, M., Brenner, C., Carroll, D. C., Divall, E., Dover, N. P., Dromey, B., Gallegos, P., Green, J. S., Hawkes, S., Hooker, C. J., Kar, S., Mckeena, P., Nagel, S. R., Najmudin, Z., Palmer, C. A. J., Prasad, R., Quinn, K. E., Rajeev, P. P., Robinson, A. P. L., Romagnani, L., Schreiber, J., Spindloe, C., Ter-Avetisyan, S., Tresca, O., Zepf, M. & Neely, D. (2011). Relativistic plasma surfaces as an efficient second generator. *N. J. Phys*. **13**, 023041.

Teubner, U., Wagner, U., Andiel, U., Pisani, F., Eidmann, K., Tsakiris, G. D., Schlegel, T., Förster, E. & Witte, K. (2004). Intense high-order harmonics generated with femtosecond laser pulses at relativistic intensities interacting with high density plasmas. *Proc. SPIE, Laser-Generated & other Lab. X-ray & EUV sources, Optics, Apps*. **5196**, 146–155.

Teubner, U., Eidmann, K., Wagner, U., Andiel, U., Pisani, F., Tsakiris, G. D., Witte, K., Meyer-Ter-vehn, J., Schlegel, T. & Förster, E. (2004). Harmonic emission from the rear side of thin overdense foils irradiated with intense ultra short laser pulses. *Phys. Rev. Lett*. **92**, 185001–4.

Tripathi, V. K., Liu, C. S., Shao, X., Eliasson, B. & Sagdeev, R. Z. (2009). Laser acceleration of monoenergetic protons in a self-organized double layer from thin foil. *Plasma Phys. Control. Fusion* **51**, 024014.

Upadhyay, A. & Tripathi, V. K. (2005). Second harmonic generation in a laser channel. *J. Plasma Phys*. **71**, 359–366.

Weber, S. & Riconda, C. (2015). Temperature dependence of parametric instabilities in the context of the shock-ignition approach to inertial confinement fusion. *High Power Laser Sci. Eng*. **3**, 1–13.

Zhang, P., Ridgers, C. P. & Thomas, A. G. R. (2015). The effect of nonlinear quantum electrodynamics on relativistic transparency and laser absorption in ultra-relativistic plasmas. *New J. Phys*. **17**, 043051.

https://doi.org/10.1017/S026303461700026X Published online by Cambridge University Press